

Soret and MHD effects on bioconvection wall jet flow of nanofluid containing gyrotactic microorganisms

Syed Tauseef Mohyud-Din¹ · Syed Zulfiqar Ali Zaidi¹

Received: 12 April 2016 / Accepted: 21 May 2016 / Published online: 3 June 2016
© The Natural Computing Applications Forum 2016

Abstract Various applications of bioconvection phenomena in the field of medicine and biotechnology boost us to present the study of laminar wall jet flow in this specific direction. For the purpose, we have considered nanofluid containing gyrotactic microorganisms in the presence of normally applied magnetohydrodynamic forces along with Soret effects. Boundary layer approximation and similarity transformation are utilized to convert governing equations into ordinary differential equations. Influence of different emerging parameters on velocity, temperature and concentration profiles of solute, nanoparticle and motile microorganisms has been investigated. The role of physical quantities like Nusselt number, Sherwood number and density number of microorganisms is also highlighted. Increase in Nusselt number and density number of motile microorganism is observed for incremental values of bioconvection Peclet number. Soret number reflects increasing effect on Nusselt number and decreasing effect on Sherwood number because solute diffusion faces resistance due to higher values of Soret number and in return decreases rate of mass transfer. Also bioconvection Rayleigh number imposes decreasing effect on density number of the motile microorganisms.

Keywords Bioconvection · Gyrotactic microorganisms · MHD · Nanofluid · Soret effect · Wall jet

1 Introduction

Choi [1] was the first who define the suspension of tiny solid particles of size 1–100 nm in a liquid, as nanofluid. It was the breakthrough in the field of heat transfer. Das et al. [2] presented the detailed research review on nanofluids. Bioconvection is the phenomena through which the microorganisms move upward toward the surface and after increase in their density near surface; the self-propelled microorganism gets unstable and starts moving downward. Pedley et al. [3] was the one who named the said phenomena as bioconvection. They also focused their concentration to get insight of the mechanism of locomotion of the microorganisms in liquid. Wager [4] investigated and presented a detailed study about bioconvection in 1911. According to the exploration of Kuznetsov and Avramenko [5], the favorable condition for the bioconvection process within the nanofluids is that the density of nanoparticles should be so less that it will not affect the movement and direction of the microorganisms.

Separation of different size of molecules in the presence of temperature gradient gives rise to Soret effect. Also, we can observe the Dufour effect in the presence of mass gradient whenever there is heat flux in a chemical system. Soret and Dufour effects are also called as thermal-diffusion and diffusion-thermo effects, respectively. The Soret and Dufour effects on fluid flowing along vertical plate with variable viscosity under free convection were investigated by Elbashbeshy and Ibrahim [6]. The study on boundary layer flow for convection along with Soret and Dufour effects on temperature-based viscosity was conducted by Kafoussias and William [7]. Yih [8] discussed variation in heat and mass transfer due to various parameters by considering the geometry of wedge with changing temperature of the wall. Discussion on heat and mass

✉ Syed Tauseef Mohyud-Din
syedtauseefs@hotmail.com

¹ Department of Mathematics, Faculty of Sciences, HITEC University, Taxila Cantt, Pakistan

transfer for non-Newtonian fluid was presented by Journah and Mujumdar [9]. Boundary layer flow for thermal-diffusion and diffusion-thermo effects in the presence of suction/injection was studied by Anghel et al. [10].

Wall jet flows have many applications in the industries like electronics, transport and paint spray, especially for cooling/heating systems. Launder [11, 12] explained many applications of laminar/turbulent wall jets. Tetervin [13] was the first one who conducted theoretical study on laminar wall jet flow. Glauert [14] obtained the closed analytical solution of boundary layer equations for incompressible laminar wall jet flow, and the results recorded by him were further used and endorsed by Bajura and Szewczyk [15]. Glauert's problem [14] was drawn-out by Merkin and Needham [16, 17], considering the cases of moving walls and suction/blowing. They discussed that the similarity solutions obtained by Glauert are possible when the lateral suction is applied through the moving surface. Riley [18] applied the Illingworth–Stewartson transformation to compressible radial wall jet. Chun and Schwarz [19] investigated the stability analysis of wall jet and concluded that the flow remains stable till the value of Reynolds number equals to 57. They also presented second unstable mode named as viscous mode of instability for modest values of Reynolds number. Many eminent researchers recorded remarkable results for heat and mass transfer by considering nanofluids, carbon nanotubes for different geometries [20–22].

In the literature, the research work regarding wall jet flow of nanofluid with bioconvection process with Soret effect has not been presented. Our aim is to investigate bioconvection phenomena with gyrotactic locomotion of microorganism by taking into consideration the Buongiorno [23] model of nanofluid with appropriate boundary conditions. A special concentration will be focused to analyze the Soret effects on temperature and concentration profiles in the presence of normally applied magnetic field. To get insight of the complex problem, the rate of heat and mass transfer will also be taken into account. To best of my knowledge, the results obtained from the present study are new.

2 Problem formulation

An incompressible Buongiorno [23] model of nanofluid with base fluid water is considered through wall jet. To analyze bioconvection phenomena of gyrotactic microorganisms, it is assumed that suspension of nanoparticles is stable and with concentration of <1 %. It is also assumed that presence of nanoparticles does not alter the swimming direction and velocity of the uniformly shaped microorganisms. Lower horizontal plate parallel to x -axis is at

temperature T_w , and an ambient temperature of the fluid is taken as T_∞ . The experimental results obtained by Sarkar et al. [24] show that microorganism actively survive up to the temperature of 42 °C. To analyze the solute concentration, we have also taken in account Soret effect. Variable magnetic field is applied normal to the flow of the fluid to record the effects on velocity, temperature and concentration profiles with the assumption that induced magnetic field is negligible. The schematic diagram of the problem is given Fig. 1.

After utilizing boundary layer approximation and said assumptions we obtained the governing equations in the form as follows [25, 26]:

$$\frac{\partial \hat{u}}{\partial \hat{x}} + \hat{v} \frac{\partial \hat{v}}{\partial \hat{y}} = 0, \quad (1)$$

$$\begin{aligned} \hat{u} \frac{\partial \hat{u}}{\partial \hat{x}} + \hat{v} \frac{\partial \hat{u}}{\partial \hat{y}} = & v_f \frac{\partial^2 \hat{u}}{\partial \hat{y}^2} - \frac{\sigma B^2(x)}{\rho_f} \hat{u} \\ & + \frac{1}{\rho_f} ((1 - C_\infty) \rho_f g (\beta_T (\hat{T} - T_\infty) + \beta_s (\hat{S} - S_\infty)) \\ & - (\rho_p - \rho_f) g (\hat{c} - C_\infty) - (\hat{n} - n_\infty) g \gamma (\rho_m - \rho_f)), \end{aligned} \quad (2)$$

Velocity components are to be defined as \hat{u} and \hat{v} in \hat{x} and \hat{y} direction, respectively. Density of nanofluid is denoted as ρ_f , v_f is the kinematics viscosity of nanofluid, σ denotes the electric conductivity, and $B(x)$ is used to represent variable magnetic field. \hat{C} , \hat{T} , \hat{S} , \hat{n} indicate the concentration of nanofluid, temperature, concentration of solute and microorganism's concentration, respectively. Thermal expansion coefficient is taken as β_T , volumetric solute expansion coefficient is denoted by β_s , and the nanoparticle's density is mentioned by ρ_p . The gravitational force and motile microorganism's average volume fraction are denoted by g and γ , respectively.

$$\hat{u} \frac{\partial \hat{T}}{\partial \hat{x}} + \hat{v} \frac{\partial \hat{T}}{\partial \hat{y}} = \alpha \frac{\partial^2 \hat{T}}{\partial \hat{y}^2} + \tau \left[D_B \frac{\partial \hat{C}}{\partial \hat{y}} \frac{\partial \hat{T}}{\partial \hat{y}} + \left(\frac{D_T}{T_\infty} \right) \left(\frac{\partial \hat{T}}{\partial \hat{y}} \right)^2 \right], \quad (3)$$

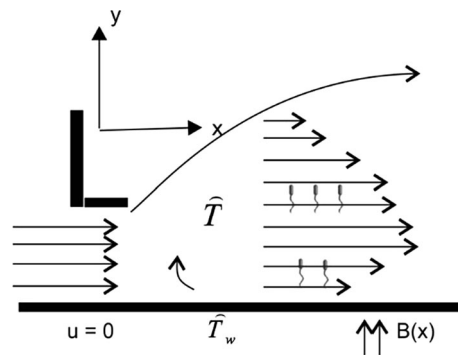


Fig. 1 Schematic diagram of problem

$$\hat{u} \frac{\partial \hat{S}}{\partial \hat{x}} + \hat{v} \frac{\partial \hat{S}}{\partial \hat{y}} = D_s \frac{\partial^2 \hat{S}}{\partial \hat{y}^2} + k_T \left(\frac{D_m}{T_\infty} \right) \frac{\partial^2 \hat{T}}{\partial \hat{y}^2}, \tag{4}$$

$$\hat{u} \frac{\partial \hat{C}}{\partial \hat{x}} + \hat{v} \frac{\partial \hat{C}}{\partial \hat{y}} = D_B \frac{\partial^2 \hat{C}}{\partial \hat{y}^2} + \left(\frac{D_T}{T_\infty} \right) \frac{\partial^2 \hat{T}}{\partial \hat{y}^2}, \tag{5}$$

$$\hat{u} \frac{\partial \hat{n}}{\partial \hat{x}} + \hat{v} \frac{\partial \hat{n}}{\partial \hat{y}} + \frac{bW_c}{(\hat{C}_w - \hat{C}_\infty)} \left(\frac{\partial \hat{n}}{\partial \hat{y}} \frac{\partial \hat{C}}{\partial \hat{y}} + \hat{n} \frac{\partial^2 \hat{C}}{\partial \hat{y}^2} \right) = D_n \frac{\partial^2 \hat{n}}{\partial \hat{y}^2}, \tag{6}$$

Thermal diffusivity of nanofluid is taken as α , D_B is used for Brownian diffusion coefficient, and D_T is the coefficient of thermophoresis diffusion. The ratio of heat capacitance of nanoparticles and base fluid is given by $\tau = \frac{(\rho C)_p}{(\rho C)_f}$, where D_s and D_m represent the coefficients of solute and mass diffusivity, respectively. With the assumption that product of b and W_c remains constant, we define b as constant of chemotaxis and W_c as the maximum speed of microorganisms. We also define D_n as coefficient of microorganisms' diffusion.

The appropriate boundary conditions are:

$$\begin{aligned} \hat{u} = 0, \hat{v} = 0, \hat{T} = T_w, \hat{C} = C_w, \hat{n} = n_w, \quad \text{at } \hat{y} = 0, \\ \hat{u} = 0, \hat{T} \rightarrow T_\infty, \hat{C} \rightarrow C_\infty, \hat{n} \rightarrow n_\infty \quad \text{at } \hat{y} \rightarrow \infty, \end{aligned} \tag{7}$$

In order to utilize numerical technique, the following similarity transforms [14, 27] are adopted:

$$\begin{aligned} \eta = \frac{\hat{y}}{v_f^{1/2} \hat{x}^{3/4}}, \quad \psi = 4\sqrt{v_f} \hat{x}^{1/4} f(\eta), \quad \theta(\eta) = \frac{\hat{T} - T_\infty}{T_w - T_\infty}, \\ \phi(\eta) = \frac{\hat{C} - C_\infty}{C_w - C_\infty}, \quad w(\eta) = \frac{\hat{S} - S_\infty}{S_w - S_\infty}, \quad \chi(\eta) = \frac{\hat{n} - n_\infty}{n_w - n_\infty} \end{aligned} \tag{8}$$

Velocity in stream function form is defined as $u = \frac{\partial \psi}{\partial \hat{y}}$ and $\hat{v} = -\frac{\partial \psi}{\partial \hat{x}}$.

Using Eq. (8) along with stream function into Eqs. (1)–(7), we obtained system of nonlinear differential equations with boundary equations as follows:

$$\begin{aligned} f''' + 2(f')^2 + ff'' + \frac{1}{4} \lambda(\theta + Nc w - Nr \phi - Rb \chi) - M^2 f' \\ = 0, \end{aligned} \tag{9}$$

$$\theta'' + Pr f \theta' + Nb \phi' \theta' + Nt \theta'^2 = 0, \tag{10}$$

$$w'' + Lnf w' + Sr \theta'' = 0, \tag{11}$$

$$\phi'' + Lef \phi' + \frac{Nt}{Nb} \theta'' = 0, \tag{12}$$

$$\chi'' + Lb(f \chi') - Pe(\phi' \chi' + \phi''(\Omega + \chi)) = 0. \tag{13}$$

The boundary conditions also transform to

$$\begin{aligned} f(0) = 0, f'(0) = 0, \theta(0) = 1, w(0) = 1, \phi(0) \\ = 1, \chi(0) = 1, \end{aligned} \tag{14}$$

$$f(\infty) = 1, \theta(\infty) = 0, w(\infty) = \phi(\infty) = 0, \chi(\infty) = 0. \tag{15}$$

The derivative w.r.t η is represented by primes.

After applying Eq. (8) we obtained following non-dimensional numbers and parameters,

$M^2 = \frac{\sigma B_0^2}{\rho_f}$: Hartmann number	$Rb = \frac{\gamma(n_w - n_\infty)(\rho_p - \rho_f)}{\beta_T \rho_f (1 - C_\infty)(T_w - T_\infty)}$: Bioconvection Rayleigh number
$Pr = \frac{\nu_f}{\alpha}$: Prandtl number	$Nc = \frac{\beta_s (S_w - S_\infty)}{\beta_T (T_w - T_\infty)}$: Regular double-diffusive buoyancy parameter
$Le = \frac{\nu_f}{D_B}$: Standard Lewis number	$Sr = \frac{D_m k_T (T_w - T_\infty)}{D_s T_\infty (S_w - S_\infty)}$: Soret number
$Nb = \frac{\tau D_B (C_w - C_\infty)}{\alpha}$: Brownian motion parameter	$Ln = \frac{\nu_f}{D_s}$: Nanofluid Lewis number
$Nt = \frac{\tau D_T (T_w - T_\infty)}{T_\infty \alpha}$: Thermophoresis parameter	$Nr = \frac{(C_w - C_\infty)(\rho_p - \rho_f)}{\beta_T \rho_f (1 - C_\infty)(T_w - T_\infty)}$: Buoyancy ratio parameter
$\lambda = \frac{Gr_x}{Re_x^2}$: Ratio of Grashof and Reynolds number	$Pe = \frac{bW_c}{D_n}$: Bioconvection Peclet number
$Gr_x = \frac{g \beta_T (1 - C_\infty)(T_w - T_\infty) x^3 / v_f^2}{x / v_f^2}$: Grashof number	$Re_x = \frac{x^{1/2}}{v_f}$: Reynolds number
$Lb = \frac{\nu_f}{D_n}$: Bioconvection Lewis number	$\Omega = \frac{n_\infty}{(n_w - n_\infty)}$: Microorganisms concentration difference parameter

The physical engineering interest quantities are local Nusselt number Nu_x , local Sherwood number Sh_x and density number of motile microorganisms Nn_x

$$Nu_x = \frac{x q_w}{k_f (T_w - T_\infty)} \quad \text{where} \quad q_w = -k_f \left(\frac{\partial \hat{T}}{\partial \hat{y}} \right)_{\hat{y}=0} \tag{16}$$

$$Re_x^{-1/2} Nu_x = -\theta'(0),$$

$$Sh_x = \frac{x q_m}{D_B (C_w - C_\infty)} \quad \text{where} \quad q_m = -D_B \left(\frac{\partial \hat{C}}{\partial \hat{y}} \right)_{\hat{y}=0}$$

$$Re_x^{-1/2} Sh_x = -\phi'(0), \tag{17}$$

$$Nn_x = \frac{x q_n}{D_n (n_w - n_\infty)} \quad \text{where} \quad q_n = -D_n \left(\frac{\partial \hat{n}}{\partial \hat{y}} \right)_{\hat{y}=0} \tag{18}$$

$$Re_x^{-1/2} Nn_x = -\chi'(0).$$

3 Numerical procedure

To obtain numerical solution of the problem, we have utilized boundary layer approximation and similarity transformation. The obtained solution of set of ordinary

differential equations along with boundary conditions we used Runge–Kutta method coupled with shooting method. In order to calculate results in efficient and speedy manner, we extended the support of software like Mathematica 10 in our research work. To obtain the meaningful results and order of convergence at 10^{-7} , we select the interval size $\Delta\eta = 0.001$. To get insight of the problem, the influence of various parameters on velocity, temperature and concentration profiles of nanoparticles and microorganism has also been recorded.

4 Results and discussion

Figures 2, 3, 4, 5 and 6 represent the analysis of velocity distribution under effect of parameters that arise due to nanofluid and bioconvection phenomena. From Figs. 2 and 3, we have observed rise in velocity for increasing values of λ (ratio of Grashof number to Reynolds number) and N_c (regular double-diffusive buoyancy parameter). As we know that double-diffusive means occurrence of heat and mass transfer due to thermal buoyancy, now increasing N_c leads to higher solute volumetric expansion as compared to thermal volumetric expansion. So resistance between fluid layers decreases which in result give rise to velocity distribution. Figure 4 depicted that magnetic field normal to flow produces tendency to resist the flow due to increase in Lorentz drag force. The Hartmann number is taken as controlling parameter because by increasing its value we have observed decrease in velocity profile in normalized manner. Figure 5 shows that increase in buoyancy parameter produces retardation in velocity which in return decreases the momentum boundary layer thickness. Also higher values of bioconvection Rayleigh (R_b) in Fig. 6 show interesting behavior toward velocity distribution. Due to the property of the bioconvection plumes of opposing upward motion of nanofluid because of its downward concentration, the velocity profile decreases along with momentum boundary layer thickness.

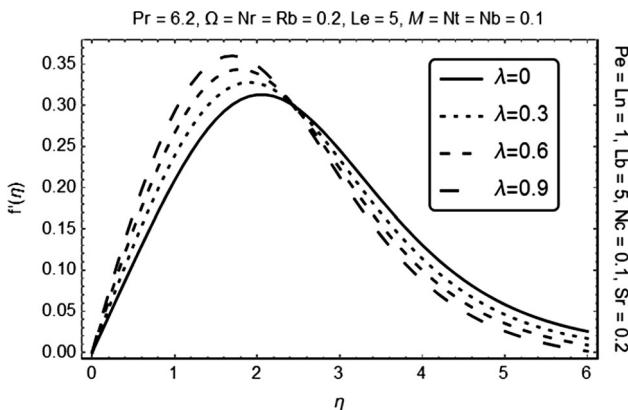


Fig. 2 Influence of λ on velocity distribution

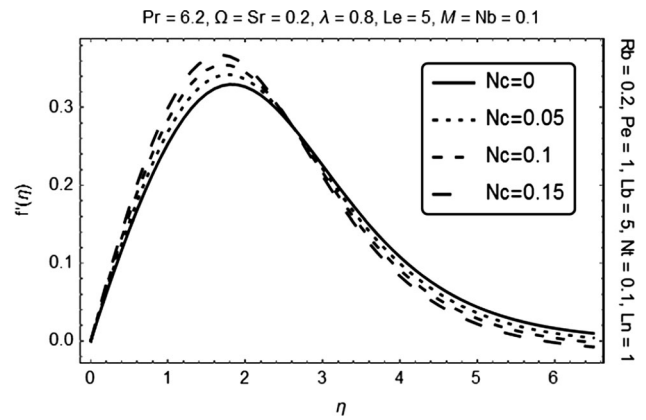


Fig. 3 Influence of N_c on velocity distribution

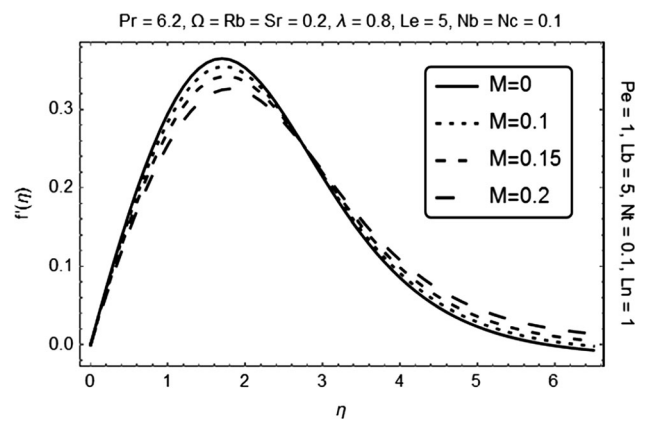


Fig. 4 Influence of M on velocity distribution

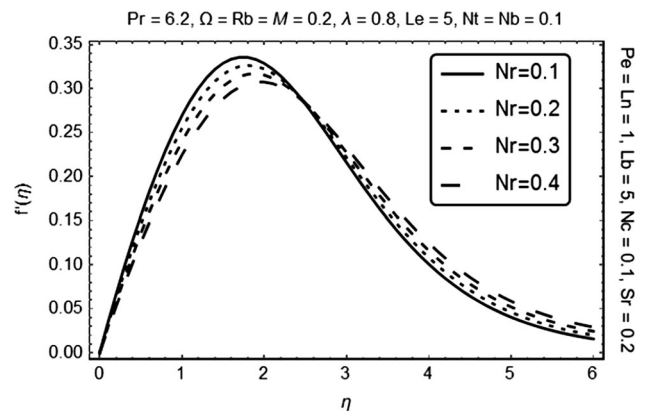


Fig. 5 Influence of N_r on velocity distribution

From Fig. 7, it is easy to understand that increased friction between the fluid layers in the presence of Lorentz force tends to raise the temperature profile. Figures 8, 9 and 10 recorded increase in temperature distribution for incremental values of thermophoresis parameter (N_t), Brownian motion parameter (N_b) and buoyancy ratio parameter (N_r). In all of the cases a rapid collision between

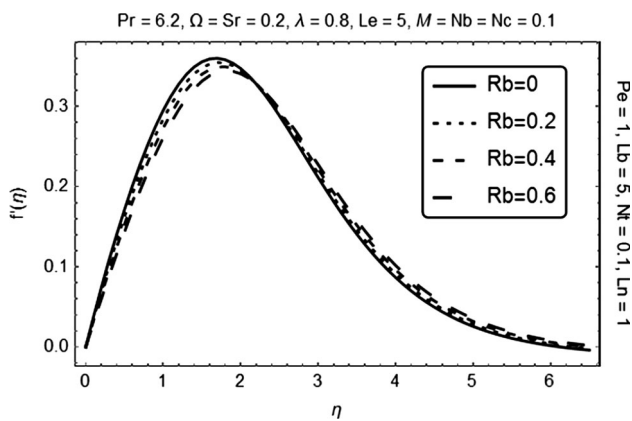


Fig. 6 Influence of Rb on velocity distribution

the molecules increases the kinetic energy which in return increases the overall temperature distribution and thermal boundary layer thickness. For higher value of buoyancy ratio parameter, we have to decrease the value of Reynolds number, which means to increase friction between the fluid layers, as it is known thing that resistance in flow tends to increase in temperature.

Analysis of nanoparticles concentration is given in Figs. 11, 12, 13, 14 and 15. It has been observed that nanoparticles volume fraction decreases for higher value of Lewis number (Le), Brownian motion parameter (Nb) and Soret number (Sr), whereas it increases by considering different incremental values of buoyancy ratio parameter (Nr) and thermophoresis parameter (Nt). When mass diffusion is less than thermal diffusion, then overall Lewis number increases which results decrease in nanoparticle concentration. Similarly, for higher values of Brownian motion parameter the collision among the molecules will be faster which in response reduces the nanoparticle concentration and boundary layer thickness. From Fig. 14, an interesting behavior of nanoparticle concentration has been observed for higher values of buoyancy ratio parameter (Nr). Within the interval $0 \leq \eta \leq 0.7$ and $\eta > 3.2$, a

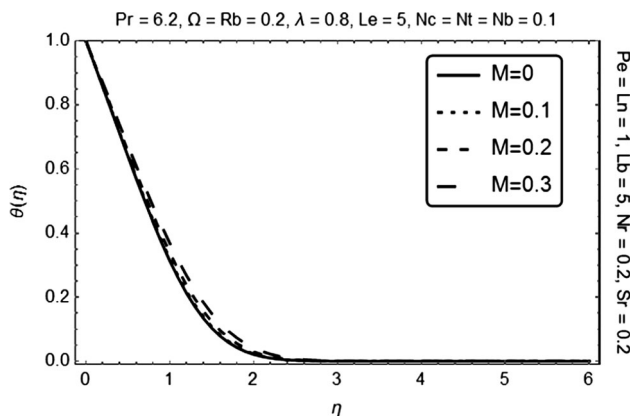


Fig. 7 Influence of M on temperature distribution

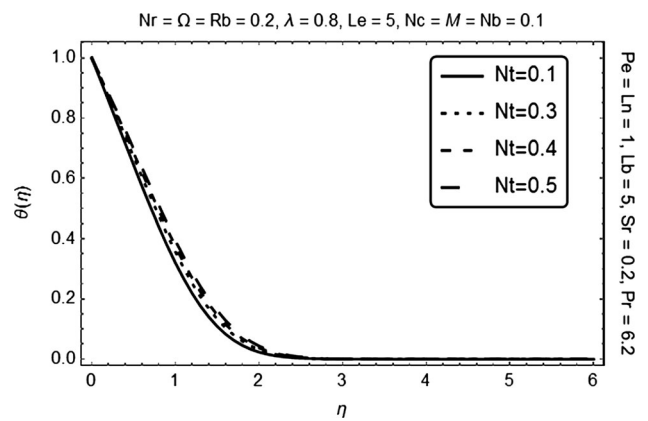


Fig. 8 Influence of Nt on temperature distribution

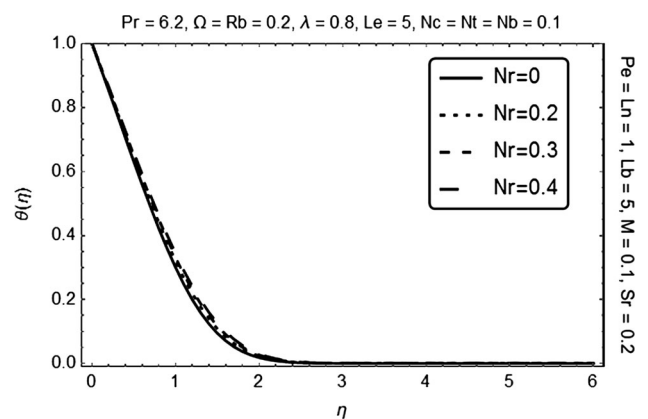


Fig. 9 Influence of Nr on temperature distribution

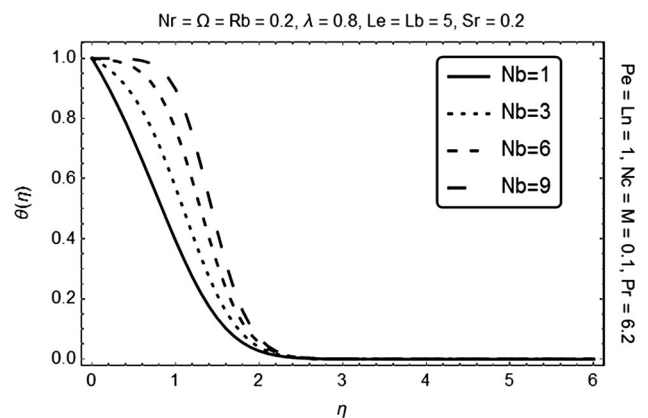


Fig. 10 Influence of Nb on temperature distribution

negligible increase in nanoparticle concentration is obtained, whereas for $0.7 < \eta \leq 3.2$, a remarkable increase is represented. Also Fig. 15 depicted that for increasing values of thermophoresis parameter, a rapid rise in nanoparticle concentration is recorded near the all due to heated plate.

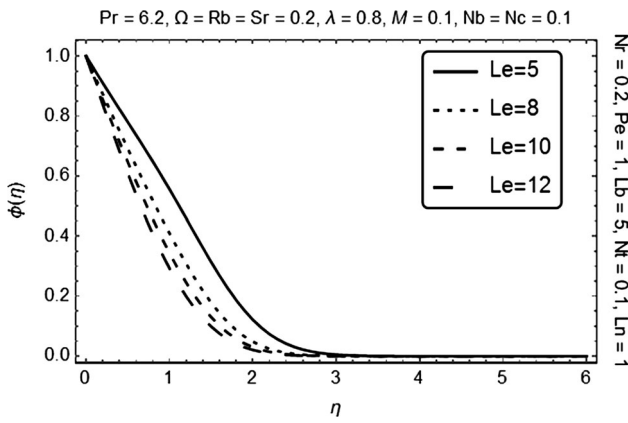


Fig. 11 Influence of Le on nanofluid concentration profile

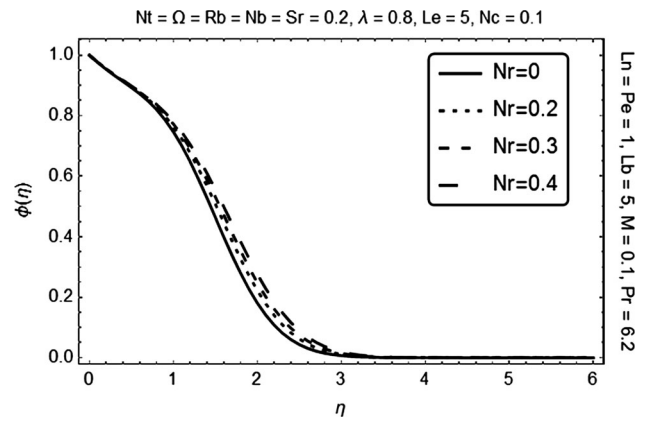


Fig. 14 Influence of Nr on nanofluid concentration profile

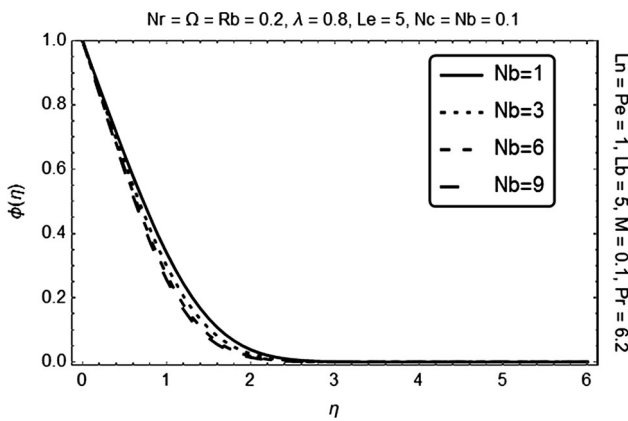


Fig. 12 Influence of Nb on nanofluid concentration profile

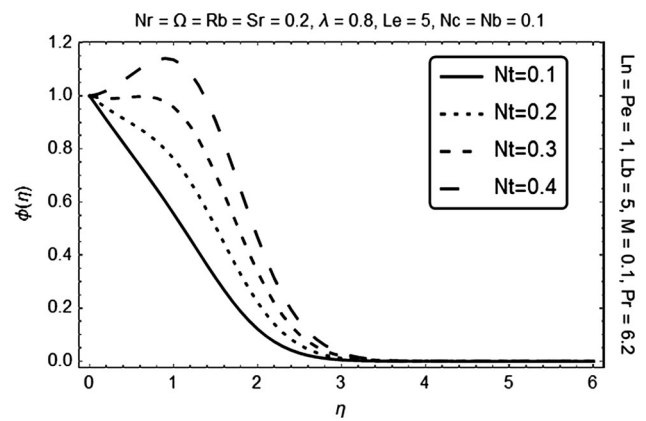


Fig. 15 Influence of Nt on nanofluid concentration profile

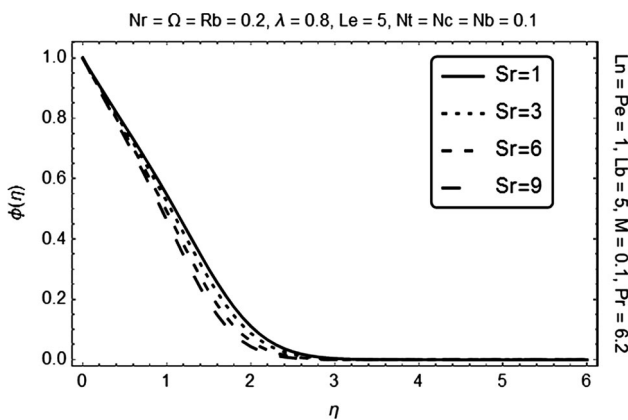


Fig. 13 Influence of Sr on nanofluid concentration profile

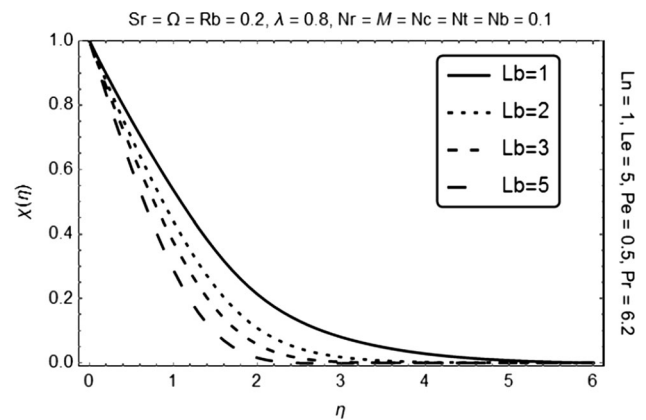


Fig. 16 Influence of Lb on microorganism concentration profile

A strong influence of different parameters on motile microorganism's concentration can be observed in Figs. 16, 17, 18, 19 and 20. Due to high diffusion rate for increasing value of bioconvection Lewis number (Lb), the surface velocity reduces which tends toward decline of the microorganism's concentration layer thickness, as shown

in Fig. 16. From Fig. 17, it is recorded that for higher values of Brownian motion parameter (Nb), the density of microorganisms reduces due to rapid collision of molecules. The speed of the microorganisms is controlled and increases directly with help of bioconvection Peclet number (Pe). Figure 18 represents that by giving increment in

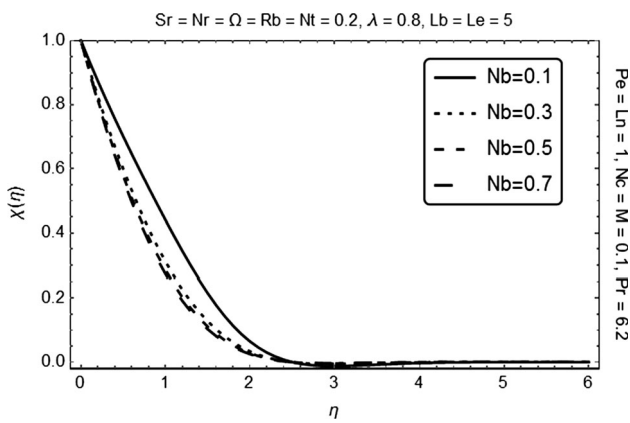


Fig. 17 Influence of Nb on microorganism concentration profile

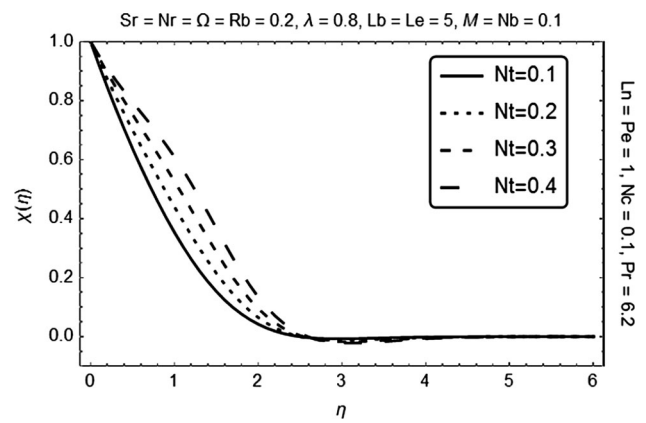


Fig. 20 Influence of Nt on microorganism concentration profile

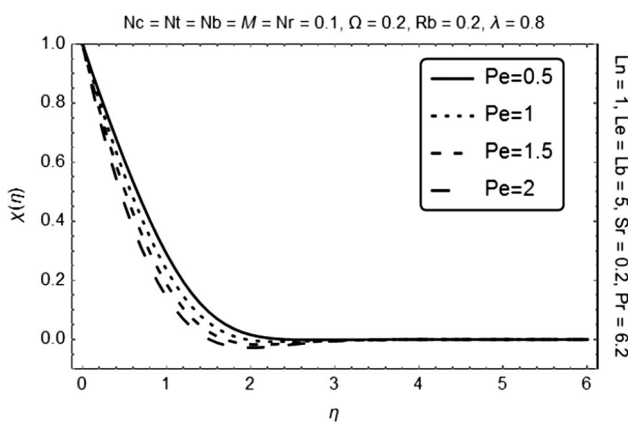


Fig. 18 Influence of Pe on microorganism concentration profile

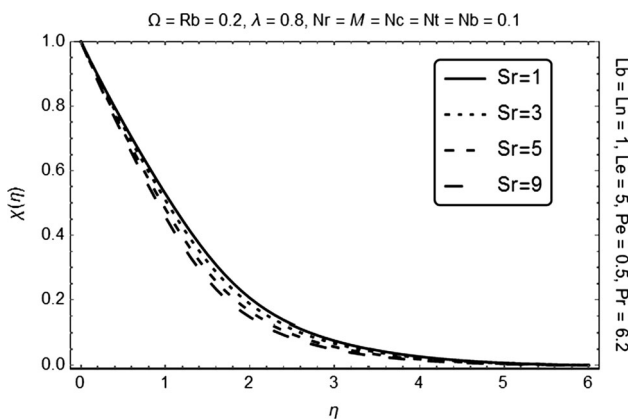


Fig. 19 Influence of Sr on microorganism concentration profile

the values of Pe we observed reduction in microorganism’s concentration close to the surface.

The impact of Soret effect can be observed in Fig. 19. The density of the motile microorganism decreases for rising values of Soret number. The low mass diffusion always tends to stronger thermophoresis effects which mean higher values of thermophoresis parameter Fig. 20,

helps to increase the concentration profile of motile microorganisms. Figure 21 illustrated decrease in solute concentration for higher values of nanofluid Lewis number (Ln). For Ln = 1, we have observed a rapid increase in solute concentration for interval $0 \le \eta \le 1.2$ and then gradual decrease. Reduction in mass diffusivity due to higher values of nanofluid Lewis number results in reduction in solute concentration boundary layer thickness. In the presence of Lorentz viscous drag, the velocity of fluid reduces because of friction between the fluid layers which in turn increases the solute concentration, as shown in Fig. 22. Also it is known that Soret effect decreases the temperature gradient which helps in enhancing the solute concentration boundary layer thickness as shown in Fig. 23.

Influence of various parameters on rate of heat of transfer is presented in Figs. 24, 25, 26 and 27. Since increase in advective transport rate leads to rise in rate of heat transfer, an increasing and converging effect of bioconvection Peclet number in the presence of bioconvection Lewis number on Nusselt number is shown in Fig. 24. With nanofluid Lewis number (Ln), the influence of Soret number (Sr) on Nusselt number is shown in Fig. 25. It has

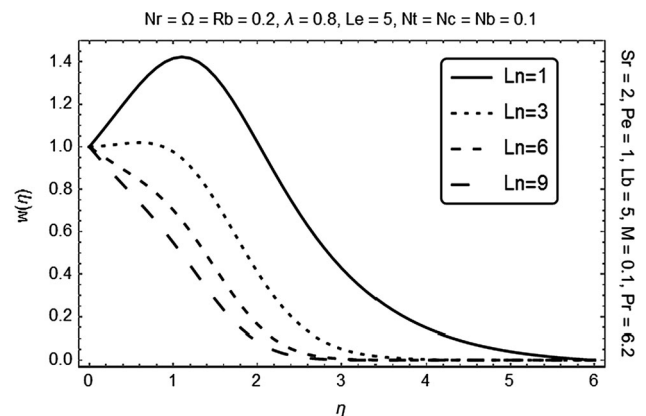


Fig. 21 Influence of Ln on solute concentration profile

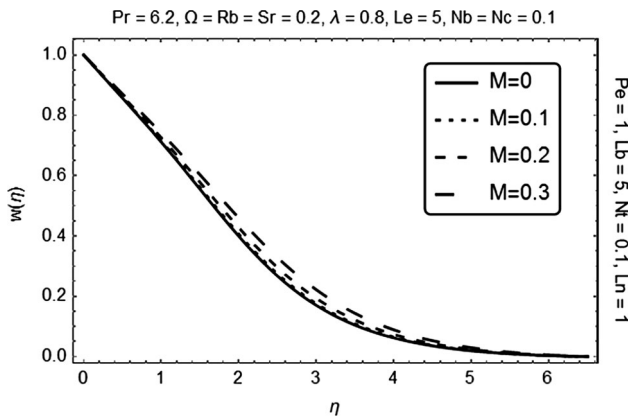


Fig. 22 Influence of M on solute concentration profile

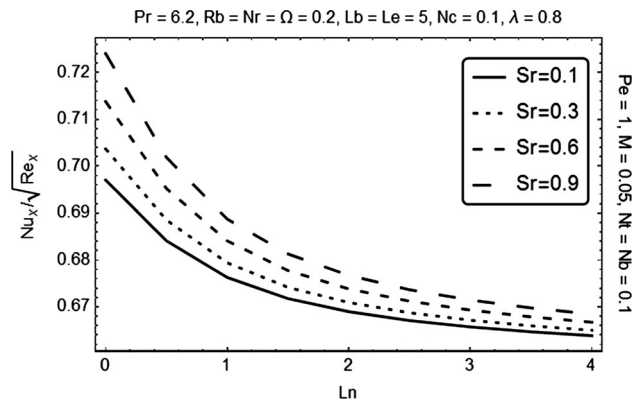


Fig. 25 Effect of Sr with Ln on Nusselt number

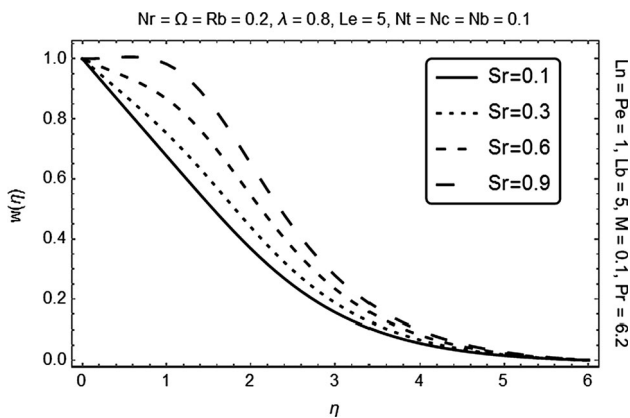


Fig. 23 Influence of Sr on solute concentration profile

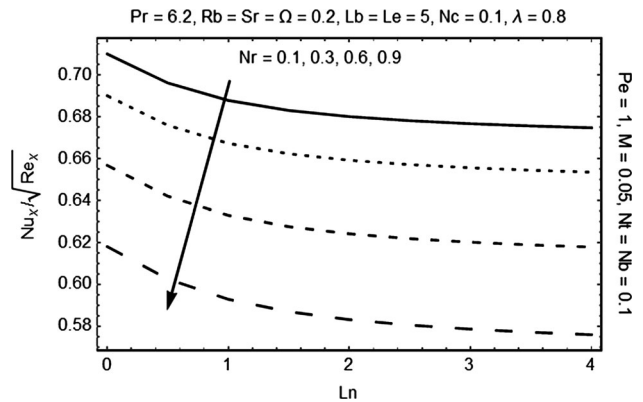


Fig. 26 Effect of Nr with Ln on Nusselt number

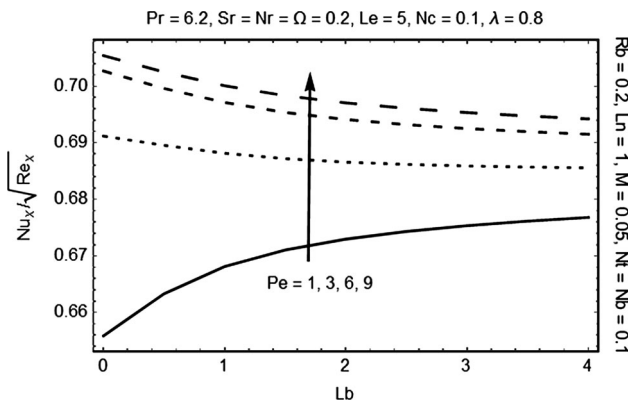


Fig. 24 Effect of Pe with Lb on Nusselt number

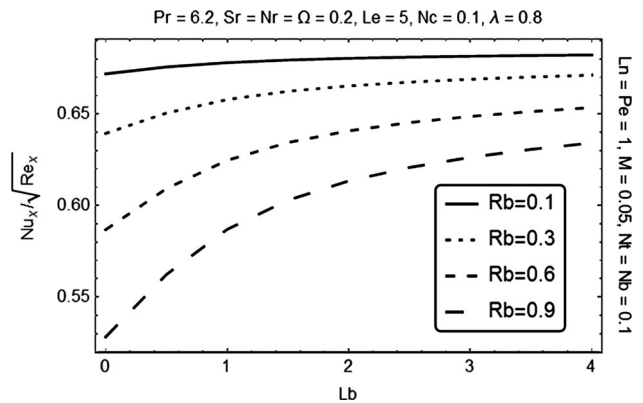


Fig. 27 Effect of Rb with Lb on Nusselt number

been observed that near the wall the rate of heat transfer is greater. Also with increased Soret number we obtained rise in Nusselt number. Figure 26 depicted that Nusselt number decreases for incremental values of buoyancy ratio parameter (Nr). Actually, increase in Nr along with nano-fluid Lewis number (Ln) helps in reducing the thermal boundary layer which in turn decreases the rate of heat

transfer near the wall. Figure 27 recorded that for increasing values of bioconvection Rayleigh number (Rb) in the presence of bioconvection Lewis number (Lb), a decrease in Nusselt number in converging manner is observed.

Analysis of rate of mass transfer is recorded through Figs. 28, 29, 30, 31 and 32 under variation of different

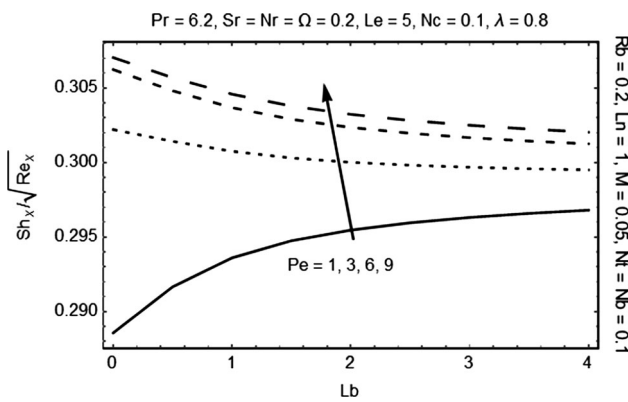


Fig. 28 Effect of Pe with Lb on Sherwood number

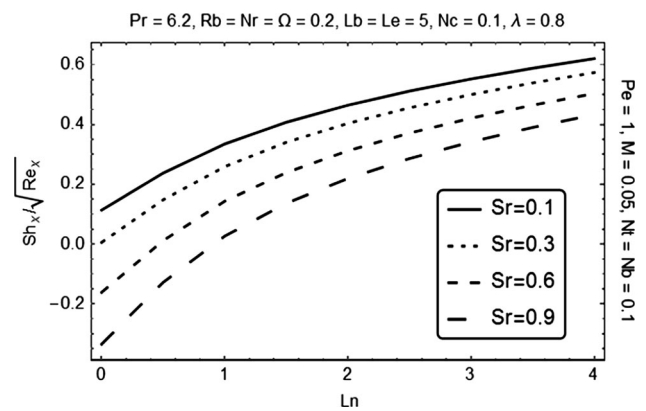


Fig. 31 Effect of Sr with Ln on Sherwood number

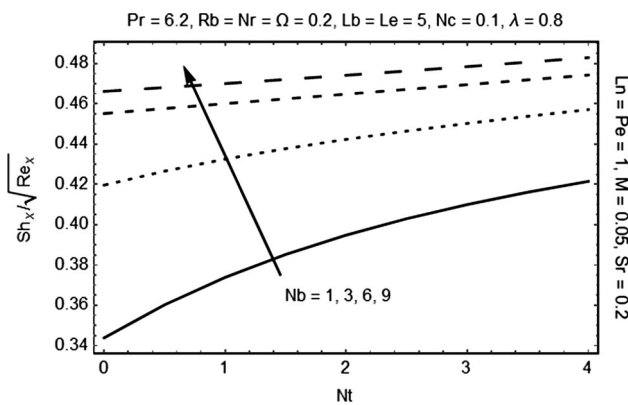


Fig. 29 Effect of Nb with Nt on Sherwood number

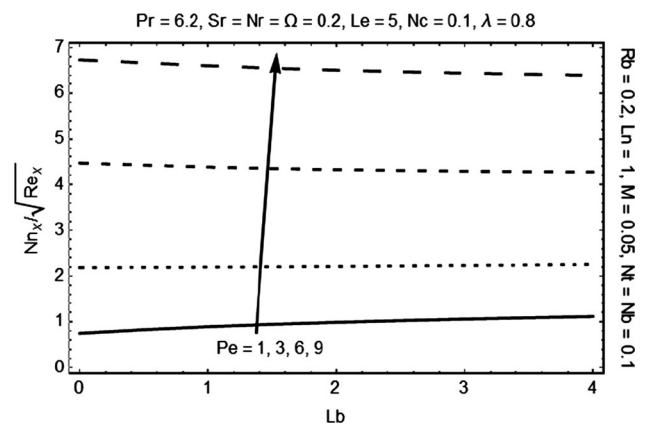


Fig. 32 Effect of Pe with Lb on density number of motile microorganism

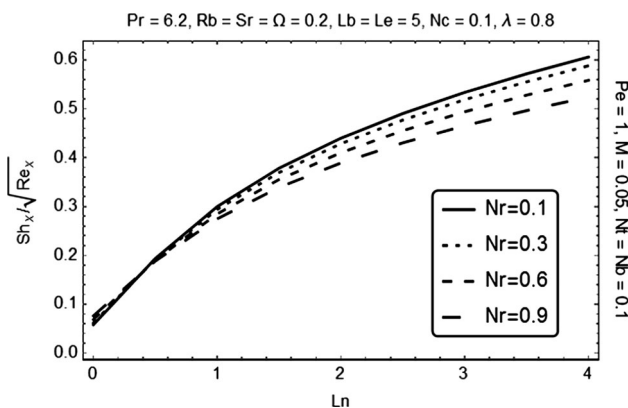


Fig. 30 Effect of Pe with Lb on Sherwood number

parameters. In Figs. 28 and 29, an increase in Sherwood number is presented by taking higher values of bioconvection Peclet number (Pe) with bioconvection Lewis number (Lb) and incremental values of Brownian motion parameter (Nb) with thermophoresis parameter (Nt). As for higher Pe, we mean increase in convected thermal energy, which in return increases the rate of mass transfer. Also increase in Brownian motion parameter tends to increase in

collision which results in increased Sherwood number. Figures 30 and 31 represent decrease in Sherwood number due to various incremental values of buoyancy ratio parameter (Nr) and Soret number (Sr). Since solute diffusion faces resistance due to higher values of Soret number and in return decreases rate of mass transfer as shown. From Fig. 31, it is recorded that for the interval $0 \leq \eta \leq 0.4$, a little rise in Sherwood number has been observed for increasing values of buoyancy ratio parameter with nanofluid Lewis number whereas, after $\eta > 0.4$, it decreases.

Influence of various parameters on local density number of motile microorganisms is presented in Figs. 32, 33 and 34. It is known that dependency of density of microorganisms is on the concentration of nanoparticles. From Fig. 32, we have observed that for different incremental values of bioconvection Peclet number (Pe), the density number of gyrotactic microorganisms increases with bioconvection Lewis number due to higher convected thermal energy. Figure 33 reveals that by increasing the bioconvection Rayleigh number in the presence of bioconvection Lewis number the density number of motile

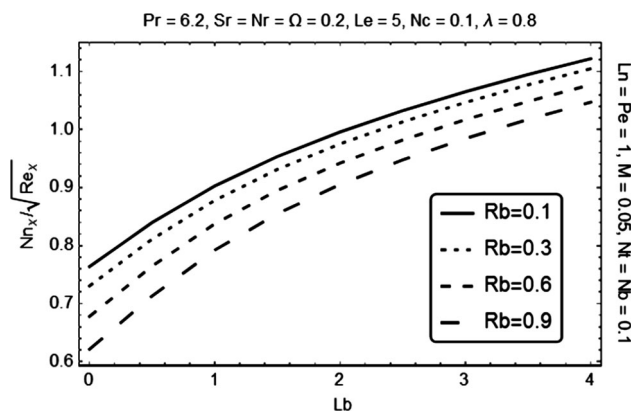


Fig. 33 Effect of Rb with Lb on density number of motile microorganism

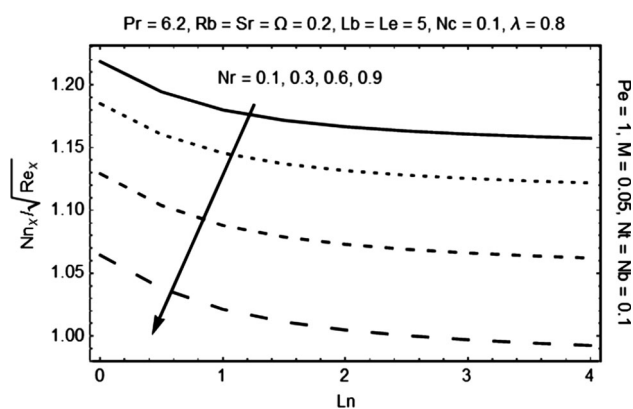


Fig. 34 Effect of Nr with Ln on density number of motile microorganism

microorganisms decreases. A strong buoyancy force in the presence of nanofluid Lewis number leads to decrease in density number of microorganisms as shown in Fig. 34.

5 Conclusion

By considering the wall jet flow of bioconvection gyrotactic microorganisms through incompressible nanofluid under the influence of MHD applied normal to the flow, we have investigated the effects of various parameters on velocity, temperature and concentration profiles. To solve numerically, the governing equations along with appropriate boundary conditions are reduced to ordinary differential equations by utilizing similarity transformation. A graphical representation is used to get more realistic picture of the problem. Following conclusions have been drawn:

1. Regular double-diffusive buoyancy parameter leads to higher solute volumetric expansion as compared to thermal volumetric expansion which results in increase in velocity distribution. Similarly,

Hartmann number is used as controlling parameter to normalize the velocity profile.

2. The buoyancy ratio parameter produces retardation in velocity of the flow which in return decreases the momentum boundary layer thickness.
3. Increase in temperature distribution is recorded for incremental values of thermophoresis parameter, Brownian motion parameter and buoyancy ratio parameter. In all of the cases, a rapid collision between the molecules increases the kinetic energy which in return increases the overall temperature distribution and thermal boundary layer thickness.
4. It has been observed that nanoparticles volume fraction decreases for higher value of Lewis number, Brownian motion parameter and Soret number, whereas it increases by considering different incremental values of buoyancy ratio parameter and thermophoresis parameter.
5. For higher values of buoyancy ratio parameter, within the interval $0 \leq \eta \leq 0.7$ and $\eta > 3.2$, a negligible increase in nanoparticle concentration is obtained, whereas for $0.7 < \eta \leq 3.2$ a remarkable increase is represented
6. Due to high diffusion rate for increasing value of bioconvection Lewis number, the surface velocity reduces which tends toward decline in the microorganism's concentration layer thickness. Also we have recorded that for higher values of Brownian motion parameter, the density of microorganisms reduces due to rapid collision of molecules.
7. Decreasing impact of Soret number is observed on density of the motile microorganism. Higher values of thermophoresis parameter help to increase the concentration profile of motile microorganisms.
8. For $Ln = 1$, we have observed a rapid increase in solute concentration for interval $0 \leq \eta \leq 1.2$ and then gradual decrease. Also effect of Soret number decreases the temperature gradient which helps in enhancing the solute concentration boundary layer thickness.
9. Nusselt number rises due to increase in bioconvection Peclet number in the presence of bioconvection Lewis number. With nanofluid Lewis number, the influence of Soret number is observed greater near the wall on Nusselt number. Also for increasing values of bioconvection Rayleigh number in the presence of bioconvection Lewis number, a decrease in Nusselt number in converging manner is observed.
10. Since solute diffusion faces resistance due to higher values of Soret number and in return decreases rate of mass transfer. It is recorded that for the interval $0 \leq \eta \leq 0.4$, a little rise in Sherwood number has

been observed for increasing values of buoyancy ratio parameter with nanofluid Lewis number, whereas after $\eta > 0.4$, it decreases.

11. We have observed that for different incremental values of bioconvection Peclet number (Pe), the density number of gyrotactic microorganisms increases with bioconvection Lewis number due to higher convected thermal energy. A strong buoyancy force in the presence of nanofluid Lewis number leads to decrease in density number of microorganisms.

Acknowledgments The authors are highly grateful to the unknown referees for their valuable comments which prove helpful in improving the quality of work.

Compliance with ethical standards

Conflict of interest All authors declare that they have no conflict of interest.

References

1. Choi SUS (1995) Enhancing thermal conductivity of fluids with nanoparticles. In: International Mechanical Engineering Congress & Exposition (ed) Developments and applications of non-Newtonian flows. The American Society of Mechanical Engineers, New York, vol 99
2. Das SK, Choi SU, Yu W, Pradeep T (2007) Nanofluids: science and technology. Wiley, New Jersey
3. Pedley TJ, Kessler JO (1992) Hydrodynamic phenomena in suspensions of swimming micro-organisms. *Annu Rev Fluid Mech* 24:313–358
4. Wager H (1911) On the effect of gravity upon the movements and aggregation of *Euglena viridis*, Ehrb., and other micro-organisms. *Philos Trans R Soc Lond B Biol Sci* 201:333–390
5. Kuznetsov AV, Avramenko AA (2004) Effect of small particles on the stability of bioconvection in a suspension of gyrotactic microorganisms in a layer of finite depth. *Int Commun Heat Mass Transf* 31:1–10
6. Elbashbeshy EMA, Ibrahim FN (1993) Steady free convection flow with variable viscosity and thermal diffusivity along a vertical plate. *J Phys D* 26(12):2137–2143
7. Kafoussias NG, Williams EW (1995) Thermal-diffusion and diffusion-thermo effects on mixed freeforced convective and mass transfer boundary layer flow with temperature dependent viscosity. *Int J Eng Sci* 33(9):1369–1384
8. Yih KA (1998) Coupled heat and mass transfer in mixed convection over a wedge with variable wall temperature and concentration in porous media: the entire regime. *Int Commun Heat Mass Transf* 25(8):1145–1158
9. Jumah RY, Mujumdar A (2000) Free convection heat and mass transfer of non-Newtonian power law fluids with yield stress from a vertical flat plate in saturated porous media. *Int Commun Heat Mass Transf* 27(4):485–494
10. Anghel M, Takhar HS, Pop I (2000) Dufour and Soret effects on free convection boundary layer over a vertical surface embedded in a porous medium. *Stud Univ Babeş-Bolyai Math* 45:11–22
11. Launder B, Rodi W (1981) The turbulent wall jets. *Prog Aerosp Sci* 19:81–128
12. Launder B, Rodi W (1983) The turbulent wall jets—measurements and modeling. *Annu Rev Fluid Mech* 15:429–459
13. Tetervin N (1948) Laminar flow of a slightly viscous incompressible fluid that issues from a slit and passes over a flat plate. National Advisory Committee for Aeronautics, Washington
14. Glauert MB (1956) The wall jet. *J Fluid Mech* 16:625–643
15. Bajura R, Szewczyk A (1970) Experimental investigation of a laminar two-dimensional plane wall-jet. *Phys Fluids* 13:1653–1664
16. Merkin J, Needham D (1986) A note on the wall-jet problem I. *J Eng Math* 20:21–26
17. Merkin J, Needham D (1987) A note on the wall-jet problem II. *J Eng Math* 21:17–22
18. Riley N (1958) Effects of compressibility on a laminar wall jet. *J Fluid Mech* 4:615–628
19. Chun D, Schwarz W (1967) Stability of the plane incompressible viscous wall jet subjected to small disturbances. *Phys Fluids* 10:911–915
20. Mohyud-Din ST, Zaidi ZA, Khan U, Ahmed N (2015) On heat and mass transfer analysis for the flow of a nanofluid between rotating parallel plates. *Aerosp Sci Technol* 46:514–522
21. Khan U, Ahmed N, Mohyud-Din S (2016) Thermo-diffusion, diffusion-thermo and chemical reaction effects on MHD flow of viscous fluid in divergent and convergent channels. *Chem Eng Sci* 141:17–27
22. Zaidi S, Mohyud-Din S (2016) Convective heat transfer and MHD effects on two dimensional wall jet flow of a nanofluid with passive control model. *Aerosp Sci Technol* 49:225–230
23. Buongiorno J (2006) Convective transport in nanofluids. *ASME J Heat Transf* 128(3):240–250
24. Sarkar AK, Georgiou G, Sharma M (1994) Transport of bacteria in porous media: I. An experimental investigation. *Biotechnol Bioeng* 44:489–497
25. Kuznetsov AV, Nield DA (2010) Natural convective boundary-layer flow of a nanofluid past a vertical plate. *Int J Therm Sci* 49(2):243–247
26. Moorthy MBK, Senthilvadivu K (2012) Soret and Dufour effects on natural convection flow past a vertical surface in a porous medium with variable viscosity. *J Appl Math*. Article ID 634806
27. Raees A, Xu H, Haq MR (2014) Explicit solutions of wall jet flow subject to a convective boundary condition. *Bound Value Prob* 2014:163